MOLEKUL
www.jmolekul.com

Articles

https://doi.org/10.20884/1.jm.2021.16.2.715

Computational Study of Scorpion Venom (*Lychas Mucronatus*) Activity as Antimicrobial Peptides (AMPs) to the SARS-CoV-2 Main Protease for the Future Coronavirus Disease (COVID-19) Inhibitors

Taufik Muhammad Fakih*

Department of Pharmacy, Faculty of Mathematics and Natural Sciences, Universitas Islam Bandung,
Jl. Rangga Gading No. 8, Bandung, 40116, Indonesia

*Corresponding author email: taufikmuhammadf@gmail.com

Received October 22, 2020; **Accepted** June 11, 2021; **Available online** July 20, 2021

ABSTRACT. The 2019 coronavirus pandemic disease (COVID-19) is still declared a global pandemic by the World Health Organization (WHO). Therefore, an effort that is considered effective in finding therapeutic agents is needed to prevent the spread of COVID-19 infection. One of the steps that can be chosen is by utilizing antimicrobial peptides (AMPs) from animal venom by targeting the specific receptor of SARS-CoV-2, namely the main protease (Mpro). Through this research, a computational approach will be conducted to predict antiviral activity, including protein-peptide docking using PatchDock algorithm, to identify, evaluate, and explore the affinity and molecular interactions of four types of antimicrobial peptides (AMPs), such as Mucroporin, Mucroporin-M1, Mucroporin-S1, and Mucroporin-S2 derived from scorpion venom (*Lychas mucronatus*) against main protease (Mpro) SARS-CoV-2. These results were then confirmed using protein-peptide interaction dynamics simulations for 50 ns using Gromacs 2016 to observe the molecular stability to the binding site of SARS-CoV-2 Mpro. Based on protein-peptide docking simulations, it was proven that the Mucroporin S-1 peptides have a good affinity against the active site area of SARS-CoV-2 Mpro, with an ACE score of −779.56 kJ/mol. Interestingly, Mucroporin-S1 was able to maintain the stability of its interactions based on the results of RMSD, RMSF, and MM/PBSA binding free energy calculations. The results of the computational approach predict that the Mucroporin-S1 peptide is expected to be useful for further research in the development of new antiviral-based AMPs for the COVID-19 infectious disease.

Keywords: COVID-19, SARS-CoV-2 Mpro, scorpion venom, antimicrobial peptides (AMPs), computational approach

INTRODUCTION

Coronaviruses (CoVs) are a large family of single-stranded RNA viruses that infect animals and also humans and can cause several diseases in various system organs of the body, such as gastrointestinal, respiratory, hepatic, and neurology (Weiss, & Leibowitz, 2011). Coronaviruses are divided into four major groups, including alpha-coronavirus, beta-coronavirus, gamma-coronavirus, and delta-coronavirus (Yang, & Leibowitz, 2015). Nowadays, six types of coronaviruses infect humans (HCoV) and have been identified, including alpha-CoVs HCoVs-NL63 and HCoVs-229E and the beta-CoVs HCoVs-OC43, HCoVs-HKU1, severe acute respiratory syndrome-CoV (SARS-CoV) (Drosten, Günther, & Preiser, 2003), and Middle East respiratory syndrome-CoV (MERS-CoV) (Zaki, Boheemen, Bestebroer, Osterhaus, & Fouchier, 2012). New coronaviruses appear regularly in humans, mainly because of the high prevalence and widespread of coronaviruses; great genetic diversity and frequent genome recombination; and increased interface activity between humans and animals (Cui, Li, & Shi, 2019; Zhu et al., 2020).

At the end of December 2019, several local health authorities reported groups of patients with pneumonia whose cause was unknown and were epidemiologically linked to the seafood market in Wuhan, Hubei Province, China (Zhu et al., 2020). SARS-CoV-2 has been identified as a new pathogenic coronavirus which is predicted to be a major cause of these events (Li et al., 2020; Zhu et al., 2020). For this phenomenon, the World Health Organization (WHO) announced a global health emergency on 30 January 2020 (Li et al., 2020). Pandemics increased rapidly with first emergency meeting estimated the COVID-19 mortality rate to be around 4% (Jin et al., 2020). Literature search related to this COVID-19 is needed to summarize the characteristics of SARS-CoV-2 especially for diagnosis, therapy, and prevention of this infectious disease (Stoecklin et al., 2020).

Main protease (Mpro) from coronavirus can be one of the potential targets in the discovery of new antiviral

candidates. Mpro plays an important role in the proteolytic process to produce two polyproteins (pp1a and pp1ab) which are used for coronavirus replication and transcription (Ge et al., 2013; Lu et al., 2020). Previous studies revealed that SARS-CoV-2 has structural similarities with SARS-CoV including the Mpro section based on complete phylogenetic analysis of the genome (Chen et al., 2009; Letko, Marzi, Munster, 2020). Interestingly, aside from the fact that this enzyme only exists in viruses and not in humans, the high conservation of Mpro among related viruses and its importance in virus replication makes this enzyme an attractive target for potential antivirals (Walls et al., 2020; Zhang et al., 2020). In addition, because no human proteases with the known specific cleavage specificity, such inhibitors are unlikely to be toxic (Park et al., 2016; Walls et al., 2019).

Among several sources of natural products, animal venoms have revealed great potential for drug development. Even though there is a dangerous mechanism of action from these animal venoms, but it has components that are potential drugs to cure disease. It is widely reported in the literature that animal venoms are rich in antimicrobial substances and contain a variety of biologically active compounds with different chemical structures (Hmed, Serria, & Mounir, 2013). Antimicrobial peptides (AMPs) are a group of peptides with important functions in the response of innate immune hosts when attacked by pathogenic organisms, such as fungi, bacteria, and viruses that are considered the first line of defense of many organisms, including plants, insects, and vertebrates (Bahar, & Ren, 2013; Jenssen, Hamill, & Hancock, 2006).

To date, there is an increasing need to design effective antiviral candidates for SARS-CoV-2. Several AMPs that have activity against SARS-CoV, namely peptides Mucroporin, Mucroporin-M1, Mucroporin-S1, and Mucroporin-S2 which are derived from scorpion venom (*Lychas mucronatus*) (Chen et al., 2012; Hong et al., 2014; Li et al., 2011; Zhao et al., 2012). In this research, an observation will be made of the molecular interactions between the AMPs and SARS-CoV-2 Mpro. Computational studies can be used to identify, evaluate and explore the affinity of AMPs as potential inhibitors of SARS-COV-2 (Kumar, Maurya, Prasad, Bhatt, & Saxena, 2020). In particular, SARS-CoV-2 Mpro is considered a target because it is a major part of forming coronavirus characteristics. Therefore, through this research, it is expected to obtain the molecular structure of reference AMPs for the treatment of COVID-19 infection.

EXPERIMENTAL SECTION

Material

The crystal structure macromolecules used in this study were the main protease (Mpro) of SARS-CoV-2. The target macromolecules were obtained from the Protein Data Bank website (http://www.rcsb.org/pdb) with the PDB ID 6LU7. The antimicrobial peptide (AMPs) molecules used in this study was the sequencing of Mucroporin, Mucroporin-M1, Mucroporin-S1, and Mucroporin-S2 peptides derived from scorpion venom (*Lychas mucronatus*).

Instrumentation

The software used in this study includes the Windows 10 Operating System and Linux Ubuntu 18.10, MGLTools 1.5.6 with AutoDock 4.2, PatchDock, PEPFOLD 3.5, Pfeature, Chimera 1.14, BIOVIA Discovery Studio 2020, Notepad++, Gromacs 2016, g_mmpbsa package and VMD 1.9.2. The hardware used in this study was a computer with Intel (R) Core i5-8500 CPU @ 4.30GHz (6 CPUs) processor, 4096 MB RAM, 2TB hard drive, 120GB solid statedrive, and Intel HD Graphics NVIDIA GeForce GTX 1080 Ti.

Preparation of the Main Protease (Mpro) Macromolecules

The main protease (Mpro) macromolecules used in this study were Mpro from the novel coronavirus 2019 (COVID-19 or SARS-CoV-2) downloaded from Protein Data Bank (http://www.rcsb.org/pdb) with PDB ID 6LU7 (Jin et al., 2020). SARS-CoV-2 Mpro macromolecular preparation was accomplished by removing water molecules and natural ligands, adding polar hydrogen atoms, and calculating the Kollman charge using MGLTools 1.5.6 with AutoDock 4.2.

Modeling of the Antimicrobial Peptide (AMPs) Molecules

The AMPs molecule used in this study was the sequencing of Mucroporin, Mucroporin-M1, Mucroporin-S1, and Mucroporin-S2 peptides derived from scorpion venom (*Lychas mucronatus*) which had been modeled using PEPFOLD 3.5 (http://bioserv.rpbs.univ-paris-diderot.fr/ PEP-FOLD/). PEP-FOLD 3.5 is a server used for the modeling of peptide sequencing into three-dimensional conformation through de novo methods with the number of amino acids between 5 to 50 (Chavan, & Deobagkar, 2015; Thévenet et al., 2012). In addition, physico-chemical properties predictions were also demostrated to compare the characteristics of each antimicrobial peptide molecule using the Pfeature (http://webs.iiitd.edu.in/ raghava/pfeature/ hysio.php).

The results of peptide molecular modeling were used as input for protein-peptide docking simulations.

Identification of the Peptide-Binding Sites in SARS-CoV-2 Mpro

The SARS-CoV-2 Mpro macromolecules that have been prepared were then identified, evaluated, and explored binding site areas that are most responsible for antimicrobial activity using BIOVIA Discovery Studio 2020 (BIOVIA, 2020). All amino acid residues that found around the natural ligand within a spherical radius distance set were prepared for the location of peptide-protein binding in protein-peptide docking simulations.

Validation of the Protein-Peptide Docking Methods

Before a protein-peptide docking simulation was performed between the Mucroporin peptide molecules and the SARS-CoV-2 Mpro macromolecules, the method must first be validated to determine the parameters to be used in the molecular docking simulations. Method validation of molecular docking parameters was done using the re-docking method. In this process, the value of the Root Mean Square Deviation (RMSD) is limited to a maximum radius of 2 Å, and the protein-peptide method was chosen for the complex type (Bikadi & Hazai, 2009; Hevener et al., 2009).

Protein-Peptide Docking Simulations

Protein-peptide docking simulations were performed using PatchDock (Aruleba et al., 2018; Fakih, 2020; Sathya & Rajeswari, 2016). All AMPs molecules for these simulations were modeled and added hydrogen atoms from the de novo methods. Complex types were selected as protein-peptide with default clustering RMSD 2 Å. The representation of the Connolly dot surface of the molecule into different components including convex, concave, and flat patch was generated through the PatchDock algorithm. PatchDock was optimized, refined, overhauled, and reselected the side chain interface from the top 10 candidate solutions. It also changes the orientation of the molecule relative by limiting flexibility in the side chains of the interacting surface and allowing the movements of small rigid-body. Observation of the protein-peptide docking simulation results was accomplished using BIOVIA Discovery Studio 2020 (BIOVIA, 2020).

Protein-Peptide Interaction Dynamics Simulations

Molecular dynamics simulations were conducted on all protein-peptide complexes resulting from molecular docking studies. Simulations were performed using Gromacs 2016 (Pronk et al., 2013; Abraham et al., 2015; Pall et al., 2015) and simulation results were analyzed with VMD 1.9.2 (Humphrey, Dalke, & Schulten, 1996) and BIOVIA Discovery Studio 2020 (BIOVIA, 2020). AMBER99SB-ILDN and AMBER general forces fields (GAFF) were used to parameterize the SARS-CoV-2 Mpro macromolecules and Mucroporin peptide molecules (Aliev et al., 2014). The long-distance electrostatic forces are determined using the Ewald Particle Mesh method (Darden, York, & Pedersen, 1993; Essmann et al., 1995). Neutralization of the system was done by adding sodium (Na+) and chloride (Cl−) ions. The cubic TIP3P water model was used to solve complex systems. The simulation step includes minimization, heating up to 310 K, temperature equilibrium (NVT), pressure equilibrium (NPT), and the production process with a timestep of 2 fs for 50 ns. System stability was identified and evaluated by analysis of energy, temperature, pressure, Root Mean Square Deviation (RMSD), and Root Mean Square Fluctuation (RMSF) of the SARS-CoV-2 Mpro macromolecules. Analysis of the interaction stability of Mucroporin peptide molecules and SARS-CoV-2 Mpro macromolecules was carried out by calculating the residual values of RMSD and RMSF at the binding site during the simulation.

MM/PBSA Binding Free Energy Calculations

The calculation of binding free energy as a result of molecular dynamics simulations using the Molecular Mechanics Poisson-Boltzmann Surface Area (MM/PBSA) method was demonstrated using the g_mmpbsa package (Baker, Sept, Joseph, Holst, & McCammon, 2001; Kumari, & Kumar, 2014) which is integrated in the Gromacs 2016. Polar desolvation energy was calculated using the Poisson-Boltzmann equation using a grid size of 0.5 Å. The dielectric constant of the solvent was set to 80 to represent water as solvent (Hou et al., 2010; Spackova et al., 2003). The nonpolar contribution was determined by calculating the surface area accessible to the solvent with a solvent radius of 1.4 Å. The binding free energy of a protein-peptide complex was determined based on 50 snapshots taken from the beginning to the end of the molecular dynamics simulations trajectories of the complex molecule.

RESULTS AND DISCUSIONS

Protein-Peptide Docking Simulations

All modeled antimicrobial peptides (AMPs) derived from scorpion venom (*Lychas mucronatus*) were then simulated by the protein-peptide binding method to the main protease (Mpro) of SARS-CoV-2 that acts as a target macromolecule (**Figure 1**). In addition, prediction of the properties and physico-chemical characteristics of the four types of AMP molecules was also performed. **Table 1** shows that the Mucroporin-S1 and Mucroporin-S2 peptide molecules are composed of polar amino acid residues, while the Mucroporin

and Mucroporin-M1 peptide molecules are constructed with non-polar amino acid residues. Therefore, it can be predicted that each peptide molecule will occupy part of the SARS-CoV-2 Mpro based on its physico-chemical properties.

The docking simulation results show that Mucroporin, Mucroporin-M1, Mucroporin-S1, and Mucroporin-S2 have a good affinity compared to natural ligands with the active site of SARS-CoV-2 Mpro, with ACE scores of −300.83 kJ/mol, −377.19 kJ/mol, −779.56 kJ/mol, −648.52 kJ/mol, and −149.94 kJ/mol, respectively (**Table 2**). This phenomenon shows a promising sign that the four types of AMPs have strong interactions and bonds at the active site area of the target macromolecule. Thereafter, all protein-peptide docking complexes were selected for further studies using the protein-peptide interaction dynamics simulations.

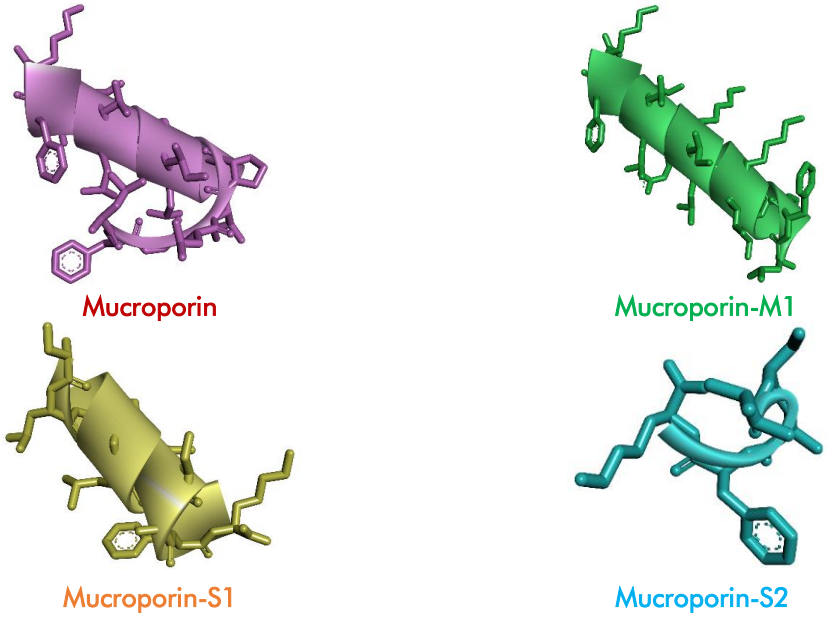

Figure 1. Structure of antimicrobial peptides (AMPs) used in this study

Table 1. Physico-chemical properties composition of antimicrobial peptides (AMPs)

Antimicrobial Peptide (AMPs)	PCP_PC	PCP_NE	PCP_PO	PCP_NP	PCP_AL	PCP_AR	PCP_BS	PCP_NE_pH
Mucroporin	0.059	0.941	0.118	0.824	0.706	0.118	0.059	0.941
Mucroporin-M1	0.294	0.706	0.118	0.588	0.471	0.118	0.294	0.706
Mucroporin-S1	0.091	0.909	0.182	0.727	0.636	0.091	0.091	0.909
Mucroporin-S2	0.200	0.800	0.200	0.600	0.400	0.200	0.200	0.800

Antimicrobial Peptide (AMPs)	PCP_HB	PCP_HL	PCP_NT	PCP_HX	PCP_TN	PCP_SM	PCP_LR
Mucroporin	0.647	0.118	0.294	0.118	0.353	0.471	0.529
Mucroporin-M1	0.588	0.294	0.118	0.118	0.176	0.235	0.765
Mucroporin-S1	0.545	0.091	0.364	0.182	0.455	0.545	0.455
Mucroporin-S2	0.6	0.2	0.2	0.2	0.4	0.6	0.4

Note: PCP_PC = positively charged residues, PCP_NE = neutral charged residues, PCP_PO = polar residues, PCP_NP = non-polar residues, PCP_AL = residues having aliphatic side chain, PCP_AR = aromatic residues, PCP_BS = basic residues, PCP_NE_pH = neutral residues based on pH, PCP_HB = hydrophobic residues, PCP_HL = hydrophilic residues, PCP_NT = neutral residues, PCP_HX = hydroxylic residues, PCP_TN = tiny residues, PCP_SM = small residues, PCP_LR = large residues.

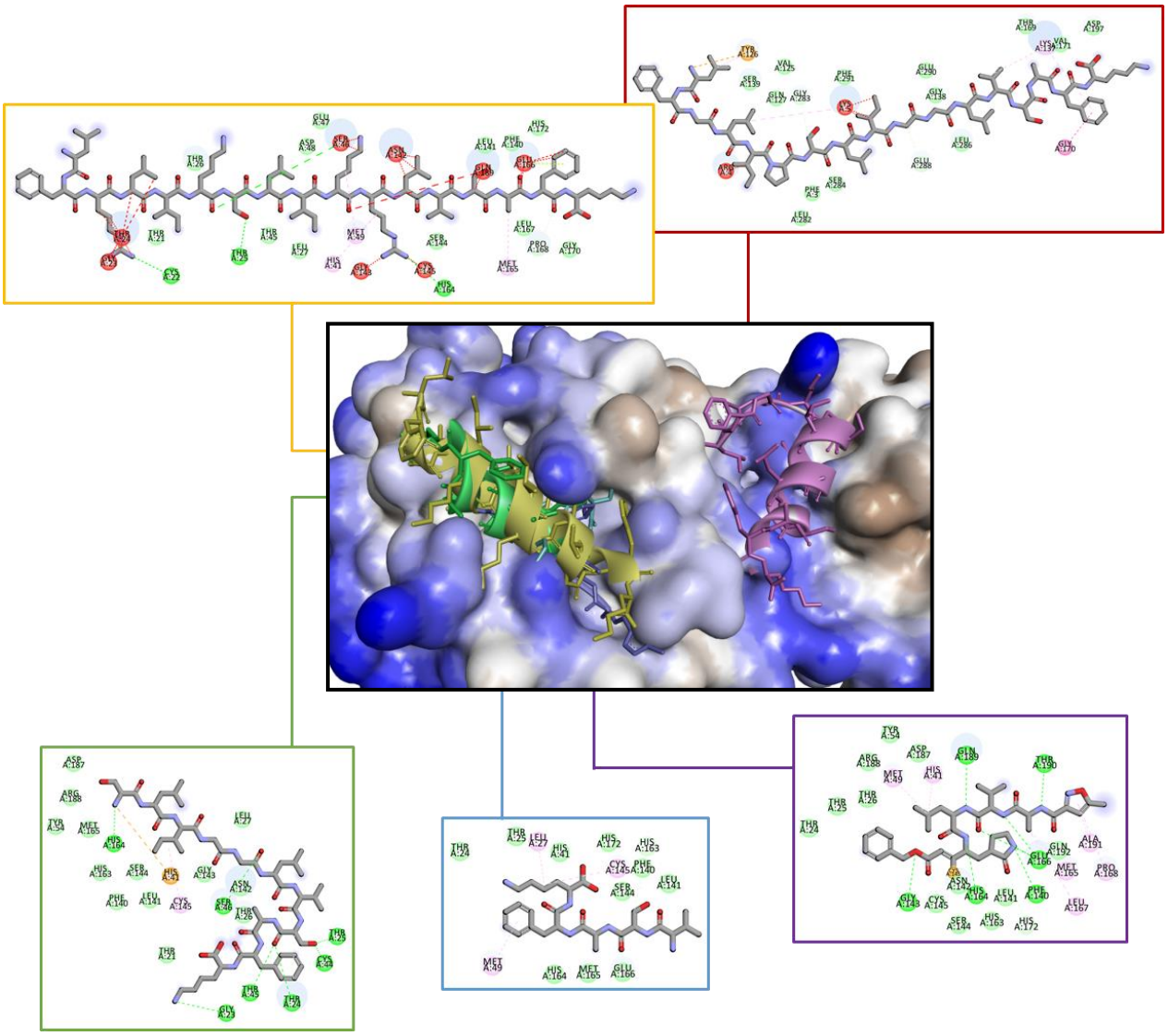

Figure 2. Overlap the protein-peptide docking pose of Mucroporin (red), Mucroporin-M1 (green), Mucroporin-S1 (yellow), Mucroporin-S2 (blue), and natural ligand (purple) binding site areas of SARS-CoV-2 Mpro

Mucroporin-S1, and Mucroporin-S2 peptides exhibit molecular interactions that were identical to SARS-CoV-2 Mpro, which were in polar patches in the active binding sites of target macromolecules (**Figure 2**). Similar to the results of the ACE score, the peptide Mucroporin-S1 has many interactions with SARS-CoV-2 Mpro including eight hydrogen bonds (with Gly23, Thr24, Thr25, Cys44, Thr45, Ser46, Asn142, and His164), one hydrophobic interaction (with Cys145), and one electrostatic interaction (with His41). Whereas the only 5 interactions that can be formed by the peptide Mucroporin-S2 include two hydrogen bonds (with Phe 140 and His163) and three hydrophobic interactions (with Leu27, Met49, and Cys145). This interaction can be formed because of hydrogen bonds, especially AMPs which act as donor hydrogen bonds and protein amino acid residues as hydrogen bond acceptors. Most hydrogen bonds between protein-peptide are quite strong, with average bond lengths in the range of 3 Å. In addition to hydrogen bonds, the interaction between the three AMPs and SARS-CoV-2 Mpro was also dominated by hydrophobic interactions and electrostatic interactions. It can be predicted that hydrogen bonds, hydrophobic interactions, and electrostatic interactions that contribute to macromolecular proteins play an important role in stabilizing protein-peptide complexes.

In contrast to other AMPs, Mucroporin attaches to the non-polar patches of the surface of SARS-CoV-2 Mpro. Moreover, the Mucroporin peptide had ten unfavorable interactions with amino acid residues at the active sites of SARS-CoV-2, including Arg4 and

Lys5. Then, although occupying the same area as the peptides Mucroporin-S1 and Mucroporin-S2, many unfavorable interactions were formed with Gly23, Thr24, Ser46, Gly143, Cys145, Asn142, Gln189, and Glu166 causing the peptide Mucroporin-M1 to have a low effect on SARS-CoV- 2 Mpro. This phenomenon shows that different conformations of the peptides Mucroporin and Mucroporin-M1 complexes can be caused by this interaction and predicted to affect their biological activity as antimicrobials.

Protein-Peptide Interaction Dynamics Simulations

After the protein-peptide complex is formed in the previous stage, further identification, evaluation, and exploration are carried out using molecular dynamics methods. The purpose of this molecular dynamics simulation is to observe the stability of each protein-peptide complex during a 50 ns simulation. The best complex stability and strong peptide bonds to SARS-CoV-2 Mpro are predicted to be able to inhibit the entry of coronavirus into cells and host tissues due to the inability to continue infection signaling. It is also important to explore visualizations, Root Mean Square Deviation (RMSD) graphs, and Root Mean Square Fluctuation (RMSF) graphs during molecular dynamics simulations.

Based on the snapshots taken at the beginning of the simulation (0 ns), 25 ns, and the end of the simulation (50 ns) it can be observed that the conformational changes of each peptide molecule generally occur when the simulation has reached 10 ns (**Figure 3**). The peptide molecule's position changes during the simulation, but significant changes are shown by the Mucroporin peptide molecule. The molecular structure of the peptide has transformed into a loop that was originally alpha-helical. Different phenomena occur in the peptide molecules Mucroporin-M1, Mucroporin S-1, and Mucroporin-S2 whose conformation does not change significantly.

The dynamics of molecular interactions between peptide molecules and their target macromolecules are studied based on simulations in solvents explicitly using Gromacs 2016. Strong affinity tends to reduce the movement of the atoms which are bound and generally stabilizes the binding site areas of SARS-CoV-2 Mpro. This phenomenon was analyzed by calculating the RMSD from the SARS-CoV-2 Mpro macromolecular binding site during the 50 ns simulation to ensure the stability and rationality of the selected conformation. The RMSD graph in **Figure 4** shows that the three systems of Mucroporin-M1, Mucroporin-S1, and Mucroporin-S2 did not have significant differences. However, similar to the visualization of snapshots during simulation, the Mucroporin peptide molecule is unable to stabilize the SARS-CoV-2 Mpro macromolecule. This is evidenced by the average RMSD value above 4 Å so that it shows a fluctuating graph after the simulation reaches 10 ns.

The RMSD data are also supported by identifying the RMSF values of amino acid residues found at the SARS-CoV-2 Mpro macromolecular binding site (**Figure 5**). However, the peptide molecules Mucroporin-M1, Mucroporin-S1, and Mucroporin-M2 were only able to bind strongly with amino acid residues at the active site of the SARS-CoV-2 Mpro macromolecule. These residues include Gly23, Thr24, Thr25, Thr26, His41, Cys44, Glu47, Met49, Asn119, Asn142, Gly143, Cys145, Met165, Glu166, Pro168, Gln189, and Ala191. Meanwhile, the Mucroporin peptide molecule moved away from the active site of SARS-CoV-2 Mpro during molecular dynamics simulations, namely interacting with the amino acid residues Ala285, Leu286, Asn277, Gly278, Arg279, Ser284, Ala285, and Leu286 (**Table 3**). High flexibility occurs around the amino acid residues found at the end of the peptide molecule because these residues play an important role in binding to the target.

MM/PBSA Binding Free Energy Calculations

Apart from identifying the visualization for each trajectory, the Root Mean Square Deviation (RMSD) graphs, and the Root Mean Square Fluctuation (RMSF) graphs, then the binding free energy calculation results from the molecular dynamics simulations from the beginning to the end of the simulations were also performed. Based on the results of the MM/PBSA calculations in **Table 4**, it can be observed that the Mucroporin-M1 and Mucroporin-S1 peptide molecules have better binding free energy compared to the Mucroporin and Mucroporin-S2 peptide molecules against the SARS-CoV-2 Mpro macromolecules.

The peptide molecules Mucroporin-M1 and Mucroporin-S1 have binding free energy values of −694.37 kJ/mol and −227.41 kJ/mol during molecular dynamics simulations. Meanwhile, the peptide molecules Mucroporin and Mucroporin-S2 have binding free energy values of −141.18 kJ/mol and −123.69 kJ/mol. Especially, the energy that contributed the most during the simulation was van der Waals interactions and electrostatic interactions. This phenomenon because the MM/PBSA approach allows observation of the influence of the contribution of van der Waals and electrostatics as well as changes in protein-peptide affinity that are influenced by the solvation process of complex systems.

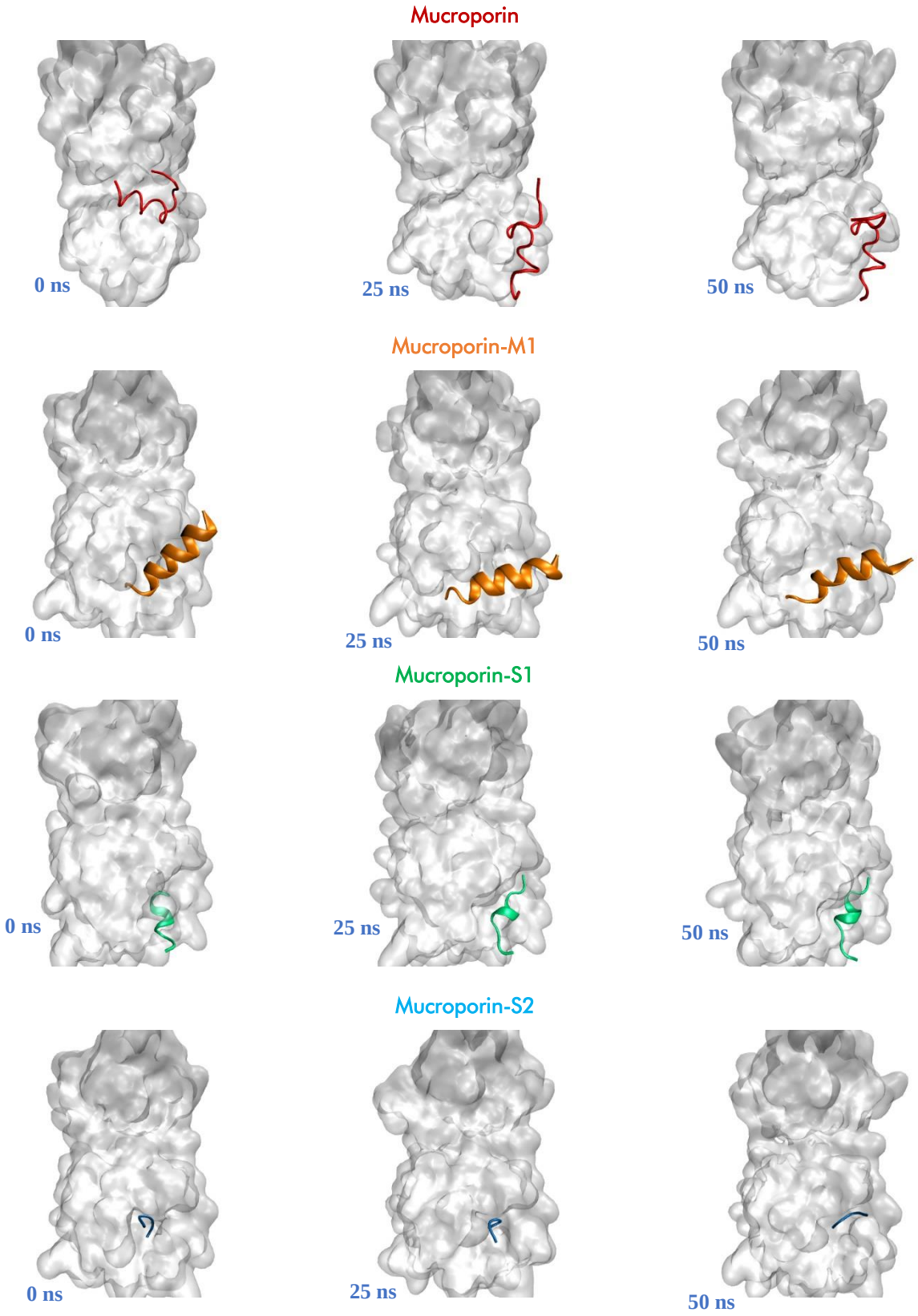

Figure 3. Snapshots of protein-peptide complex conformations during molecular dynamics simulations

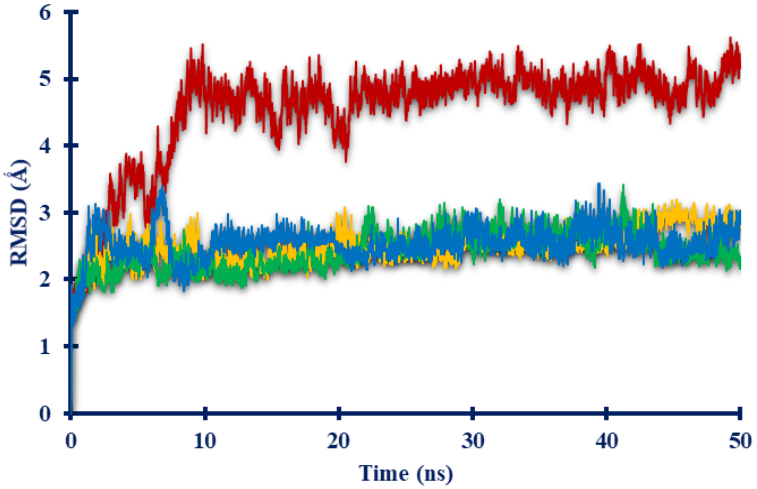

Figure 4. RMSD graphic from the complexes of SARS-COV-2 Mpro against Mucroporin (red), Mucroporin-M1 (green), Mucroporin-S1 (yellow), and Mucroporin-S2 (blue)

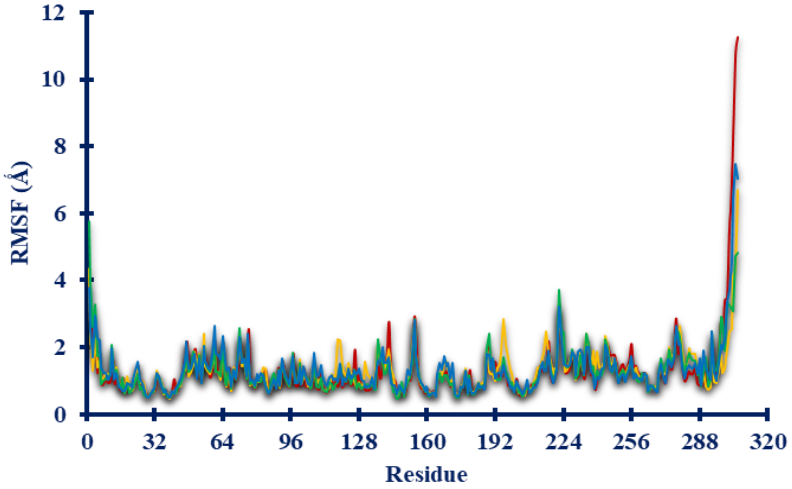

Figure 5. RMSF graphic from the complexes of SARS-COV-2 Mpro against Mucroporin (red), Mucroporin-M1 (green), Mucroporin-S1 (yellow), and Mucroporin-S2 (blue)

Table 3. Comparison of molecular interactions between molecular docking and molecular dynamics simulations

Protein-Peptide Complex	Docking Interactions	MD Interactions
Mucroporin + SARS-CoV-2 Mpro	Lys5, Tyr126, Lys137, Gly170, Tyr126, Arg4, Lys5	Ala285, Leu286, Asn277, Gly278, Arg279, Ser284, Ala285, Leu286
Mucroporin-M1 + SARS-CoV-2 Mpro	His41, Met49, Met165, Cys22, Thr25, Ser46, Glu166, Gly23, Thr24, Ser46, Asn142, Gly143, Cys145, Glu166, Gln189	His41, Met49, Cys145, Pro168, Glu47, Thr25, Thr26, Asn119, Gly143
Mucroporin-S1 + SARS-CoV-2 Mpro	Cys145, His41, Gly23, Thr24, Thr25, Cys44, Thr45, Ser46, Asn142, His164	His41, Cys44, Met49, Gly23, Thr24, His41, Cys145, Met165
Mucroporin-S2 + SARS-CoV-2 Mpro	Leu27, Met49, Cys145, Phe 140, His163	His41, Met49, Met165, Ala191, His41, His41, Asn142, Gly143, Cys145, Met165, Glu166, Gln189

Note: ■ hydrophobic interaction, ■ electrostatic interaction, ■ hydrogen bond, ■ unfavorable interaction.

Table 4. Binding free energy of protein-peptide interaction dynamics calculated by MM/PBSA

Protein-Peptide Complex	ΔE_{vdw} (kJ/mol)	ΔE_{ele} (kJ/mol)	ΔG_{PB} (kJ/mol)	ΔG_{NP} (kJ/mol)	ΔG_{Bind} (kJ/mol)
Mucroporin + SARS-CoV-2 Mpro	−171.25	−139.25	187.98	−18.66	−141.18
Mucroporin-M1 + SARS-CoV-2 Mpro	−251.28	−783.05	373.37	−33.41	−694.37
Mucroporin-S1 + SARS-CoV-2 Mpro	−233.17	−304.50	337.32	−27.07	−227.41
Mucroporin-S2 + SARS-CoV-2 Mpro	−152.09	−295.47	343.03	−19.17	−123.69

Note: ΔE_{vdw} = van der Waals contribution, ΔE_{ele} = electrostatic contribution, ΔG_{PB} = polar contribution of desolvation, ΔG_{NP} = non-polar contribution of desolvation.

CONCLUSION

Mucroporin-S1 was able to bind stably against binding site areas of SARS-CoV-2 Mpro. Interestingly, Mucroporin-S1 has the strongest affinity and interactions with the target macromolecular active site, with the ACE score of −779.56 kJ/mol. These AMPs were also able to stabilize the active site areas of the SARS-CoV-2 macromolecule during molecular dynamics simulations for 50 ns. Therefore, the results of this study indicate that Mucroporin-S1 has the potential to be further developed as SARS-CoV-2 Mpro inhibitor candidates in the treatment of COVID-19 infectious diseases.

ACKNOWLEDGEMENT

The authors thank the LPPM (Institute for Research and Community Service), Universitas Islam Bandung, for the research financially supported by the Special Research Grant Program 2020, No.039/B.04/LPPM/IV/2020.

REFERENCES

Abraham, M. J., Murtola, T., Schulz, R., Páll, S., Smith, J. C., Hess, B., & Lindahl, E. (2015). Gromacs: High performance molecular simulations through multi-level parallelism from laptops to supercomputers. *SoftwareX*, 1-2, 19-25. doi: 10.1016/j.softx.2015.06.001

Aliev, A. E., Kulke, M., Khaneja, H. S., Chudasama, V., Sheppard, T. D., & Lanigan, R. M. (2014). Motional timescale predictions by molecular dynamics simulations: Case study using proline and hydroxyproline sidechain dynamics. *Proteins: Structure, Function, and Bioinformatics*, 82(2), 195-215. doi: 10.1002/prot.24350

Aruleba, R. T., Adekiya, T. A., Oyinloye, B. E., & Kappo, A. P. (2018). Structural studies of predicted ligand binding sites and molecular docking analysis of Slc2a4 as a therapeutic target for the treatment of cancer. *International Journal of Molecular Sciences*, 19(2), 386. doi: 10.3390/ijms19020386

Bahar, A. A., & Ren, D. (2013). Antimicrobial peptides. *Pharmaceuticals*, 6(12), 1543-1575. doi: 10.3390/ph6121543

Baker, N. A., Sept, D., Joseph, S., Holst, M. J., & McCammon, J. A. (2001). Electrostatics of nanosystems: Application to microtubules and the ribosome. *Proceedings of the National Academy of Sciences USA*, 98(18), 10037-10041. doi: 10.1073/pnas.181342398

Bikadi, Z., & Hazai, E. (2009). Application of the PM6 semi-empirical method to modeling proteins enhances docking accuracy of AutoDock. *Journal of Cheminformatics*, 1(15). doi: 10.1186/1758-2946-1-15

Chavan, S. G., & Deobagkar, D. D. (2015). An in silico insight into novel therapeutic interaction of LTNF Peptide-LT10 and design of structure based peptidomimetics for putative anti-diabetic activity. *PLoS One*, 10(3), e0121860. doi: 10.1371/journal.pone.0121860

Chen, Y., Cao, L., Zhong, M., Zhang, Y., Han, C., Li, Q., Yang, J., Zhou, D., Shi, W., He, B., Liu, F., Yu, J., Sun, Y., Cao, Y., Li, Y., Li, W., Guo, D., Cao, Z., & Yan, H. (2012). Anti-HIV-1 activity of a new scorpion venom peptide derivative Kn2-7. *PLoS One*, 7(4), e34947. doi: 10.1371/journal.pone.0034947

Chen, Y., Cai, H., Pan, J., Xiang, N., Tien, P., Ahola, T., & Guo, D. (2009). Functional screen reveals SARS coronavirus nonstructural protein nsp14 as a novel cap N7 methyltransferase. *Proceedings of the National Academy of Sciences USA*, 106(9), 3484-3489. doi: 10.1073/pnas.0808790106

Cui, J., Li, F., & Shi, Z. (2019). Origin and evolution of pathogenic coronaviruses. *Nature Reviews Microbiology*, 17(3), 181-192. doi: 10.1038/s41579-018-0118-9

Darden, T., York, D., & Pedersen, L. (1993). Particle mesh Ewald: An N•log(N) method for Ewald sums in large systems. *Journal of Chemical Physics*, 98, 10089-10092. doi: 10.1063/1.464397

Dassault Systemes BIOVIA, Discovery Studio Modeling

Environment, Release 2020; Dassault Systemes: San Diego, CA, USA, 2020

Drosten, C., Günther, S., & Preiser, W. (2020). Identification of a Novel Coronavirus in Patients with Severe Acute Respiratory Syndrome. *New England Journal of Medicine*, 348(20), 1967-1976. doi: 10.1056/NEJMoa030747

Essmann, U., Perera, L., Berkowitz, M. L., Darden, T., Lee, H., & Pedersen, L. G. (1995). A smooth particle mesh Ewald method. *Journal of Chemical Physics*, 103, 8577. doi: 10.1063/1.470117

Fakih, T. M. (2020). Dermaseptin-based antiviral peptides to prevent COVID-19 through in silico molecular docking studies against SARS-Cov-2 spike protein. *Pharmaceutical Sciences and Research*, 7(Special Issue on COVID-19), 65-70. doi: 10.7454/psr.v7i4.1079

Ge, X. Y., Li, J. L., Yang, X. L., Chmura, A. A., Zhu, G., Epstein, J. H., Mazet, J. K., Hu, B., Zhang, W., Peng, C., Zhang, Y. J., Luo, C. M., Tan, B., Wang, N., Zhu, Y., Crameri, G., Zhang, S. Y., Wang, L. F., Daszak, P., & Shi, Z. L. (2013). Isolation and characterization of a bat SARS-like coronavirus that uses the ACE2 receptor. *Nature*, 503(7477), 535-538. doi: 10.1038/nature12711

Hevener, K. E., Zhao, W., Ball, D. M., Babaoglu, K., Qi, J., White, S. W., & Lee, R. E. (2009). Validation of molecular docking programs for virtual screening against dihydropteroate synthase. *Journal of Chemical Information and Modeling*, 49(2), 444-460. doi: 10.1021/ci800293n

Hmed, B., Serria, H. T., & Mounir, Z. K. (2013). Scorpion peptides: potential use for new drug development. *Journal of Toxicology*, 958797. doi: 10.1155/2013/958797

Hong, W., Li, T., Song, Y., Zhang, R., Zeng, Z., Han, S., Zhang, X., Wu, Y., Li, W., & Cao, Z. (2014). Inhibitory activity and mechanism of two scorpion venom peptides against herpes simplex virus type 1. *Antiviral Research*, 102, 1-10. doi: 10.1016/j.antiviral.2013.11.013

Hou, J. Q., Chen, S. B., Tan, J. H., Ou, T. M., Luo, H. B., Li, D., Xu, J., Gu, L. Q., & Huang, Z. S. (2010). New Insights into the structures of ligand-quadruplex complexes from molecular dynamics simulations. *Journal of Physical Chemistry B*, 114(46), 15301-15310. doi: 10.1021/jp106683n

Humphrey, W., Dalke, A., & Schulten, K. (1996). VMD: Visual molecular dynamics. *Journal of Molecular Graphics*, 14(1), 33-38. doi: 10.1016/0263-7855(96)00018-5

Jenssen, H., Hamill, P., & Hancock, R. E. (2006). Peptide antimicrobial agents. *Clinical Microbiology Reviews*, 19(3), 491-511. doi: 10.1128/CMR.00056-05

Jin, Y. H., Cai, L., Cheng, Z. S., Cheng, H., Deng, T., Fan, Y. P., Fang, C., Huang, D., Huang, L. Q., Huang, Q., Han, Y., Hu, B., Hu, F., Li, B. H., Li, Y. R., Liang, K., Lin, L. K., Luo, L. S., Ma, J., Ma, L. L., Peng, Z. Y., Pan, Y. B., Pan, Z. Y., Ren, X. Q., Sun, H. M., Wang, Y., Wang, Y. Y., Weng, H., Wei, C. J., Wu, D. F., Xia, J., Xiong, Y., Xu, H. B., Yao, X. M., Yuan, Y. F., Ye, T. S., Zhang, X. C., Zhang, Y. W., Zhang, Y. G., Zhang, H. M., Zhao, Y., Zhao, M. J., Zi, H., Zeng, X. T., Wang, Y. Y., Wang, X. H., & for the Zhongnan Hospital of Wuhan University Novel Coronavirus Management and Research Team, Evidence-Based Medicine Chapter of China International Exchange and Promotive Association for Medical and Health Care (CPAM). (2020). A rapid advice guideline for the diagnosis and treatment of 2019 novel coronavirus (2019-nCoV) infected pneumonia (standard version). *Military Medical Research*, 7, 4. doi: 10.1186/s40779-020-0233-6

Jin, Z., Du, X., Xu, Y., Deng, Y., Liu, M., Zhao, Y., Zhang, B., Li, X., Zhang, L., Peng, C., Duan, Y., Yu, J., Wang, L., Yang, K., Liu, F., Jiang, R., Yang, X., You, T., Liu, X., Yang, X., Bai, F., Liu, H., Liu, X., Guddat, L. W., Xu, W., Xiao, G., Qin, C., Shi, Z., Jiang, H., Rao, Z., & Yang, H. (2020). Structure of Mpro from COVID-19 virus and discovery of its inhibitors. *Nature*, 582(7811), 289-293. doi: 10.1038/s41586-020-2223-y

Kumar, S., Maurya, V. K., Prasad, A. K., Bhatt, M. L. B., & Saxena, S. K. (2020). Structural, glycosylation and antigenic variation between 2019 novel coronavirus (2019-nCoV) and SARS coronavirus (SARS-CoV). *Virusdisease*, 31(1), 13-21. doi: 10.1007/s13337-020-00571-5

Kumari, R., Kumar, R., Open Source Drug Discovery Consortium, & Lynn, A. (2014). g_mmpbsa—A GROMACS Tool for High-Throughput MM-PBSA Calculations. *Journal of Chemical Information and Modeling*, 54(7), 1951-1962. doi: 10.1021/ci500020m

Letko, M., Marzi, A., & Munster, V. (2020). Functional assessment of cell entry and receptor usage for lineage B β-coronaviruses, including 2019-nCoV. *Nature Microbiology*, 5(4), 562-569. doi: 10.1101/2020.01.22.915660

Li, Q., Zhao, Z., Zhou, D., Chen, Y., Hong, W., Cao, L., Yang, J., Zhang, Y., Shi, W., Cao, Z., Wu, Y., Yan, H., & Li, W. (2011). Virucidal activity of a

scorpion venom peptide variant mucroporin-M1 against measles, SARS-CoV and influenza H5N1 viruses. *Peptides*, 32(7), 1518-1525. doi: 10.1016/j.peptides.2011.05.015

Li, Q., Guan, X., Wu, P., Wang, X., Zhou, L., Tong, Y., Ren, R., Leung, K. S. M., Lau, E. H. Y., Wong, J. Y., Xing, X., Xiang, N., Wu, Y., Li, C., Chen, Q., Li, D., Liu, T., Zhao, J., Liu, M., Tu, W., Chen, C., Jin, L., Yang, R., Wang, Q., Zhou, S., Wang, R., Liu, H., Luo, Y., Liu, Y., Shao, G., Li, H., Tao, Z., Yang, Y., Deng, Z., Liu, B., Ma, Z., Zhang, Y., Shi, G., Lam, T. T. Y., Wu, J. T., Gao, G. F., Cowling, B. J., Yang, B., Leung, G. M., & Feng, Z. (2020). Early Transmission Dynamics in Wuhan, China, of Novel Coronavirus-Infected Pneumonia. *New England Journal of Medicine*, 382(13), 1199-1207. doi: 10.1056/NEJMoa2001316

Li, X., Wang, W., Zhao, X., Zai, J., Zhao, Q., Li, Y., & Chaillon, A. (2020). Transmission dynamics and evolutionary history of 2019-nCoV. *Journal of Medical Virology*, 92(5), 501-511. doi: 10.1002/jmv.25701

Lu, R., Zhao, X., Li, J., Niu, P., Yang, B., Wu, H., Wang, W., Song, H., Huang, B., Zhu, N., Bi, Y., Ma, X., Zhan, F., Wang, L., Hu, T., Zhou, H., Hu, Z., Zhou, W., Zhao, L., Chen, J., Meng, Y., Wang, J., Lin, Y., Yuan, J., Xie, Z., Ma, J., Liu, W. J., Wang, D., Xu, W., Holmes, E. C., Gao, G. F., Wu, G., Chen, W., Shi. W., & Tan, W. (2020). Genomic characterisation and epidemiology of 2019 novel coronavirus: Implications for virus origins and receptor binding. *Lancet*, 395(10224), 565-574. doi: 10.1016/S0140-6736(20)30251-8

Páll, S., Abraham, M. J., Kutzner, C., Hess, B., & Lindahl, E. (2015). Tackling exascale software challenges in molecular dynamics simulations with GROMACS In: Solving Software Challenges for Exascale. EASC 2014. Lecture Notes in Computer Science. *Solving Software Challenges for Exascale*, 3-27. doi: 10.1007/978-3-319-15976-8_1

Park, J. E., Li, K., Barlan, A., Fehr, A. R., Perlman, S., McCray, P. B., & Gallagher, T. (2016). Proteolytic processing of Middle East respiratory syndrome coronavirus spikes expands virus tropism. *Proceedings of the National Academy of Sciences U S A*, 113(43), 12262-12267. doi: 10.1073/pnas.1608147113

Prabhu, D. S., & Rajeswari, V. D. (2016). *In silico* docking analysis of bioactive compounds from Chinese medicine *Jinqi Jiangtang* Tablet (JQJTT) using Patch Dock. *Journal of Chemical and Pharmaceutical Research*, 5(8), 15-21.

Pronk, S., Páll, S., Schulz, R., Larsson, P., Bjelkmar, P., Apostolov, R., Shirts, M. R., Smith, J. C., Kasson, P. M., Spoel, D. V. D., Hess, B., & Lindahl, E. (2013). GROMACS 4.5: A high-throughput and highly parallel open source molecular simulation toolkit. *Bioinformatics*, 29(7), 845-854. doi: 10.1093/bioinformatics/btt055

Spackova, N., Cheatham, T. E., Ryjacek, F., Lankas, F., van Meervelt, L., Hobza, P., & Sponer, J. (2003). Molecular dynamics simulations and thermodynamics analysis of DNA−drug complexes. Minor groove binding between 4′,6-diamidino-2-phenylindole and DNA duplexes in solution. *Journal of the American Chemical Society*, 125(7), 1759-1769. doi: 10.1021/ja025660d

Stoecklin, S. B., Rolland, P., Silue, Y., Mailles, A., Campese, C., Simondon, A., Mechain, M., Meurice, L., Nguyen, M., Bassi, C., Yamani, E., Behillil, S., Ismael, S., Nguyen, D., Malvy, D., Lescure, F. X., Georges, S., Lazarus, C., Tabai, A., Stempfelet, M., Enouf, V., Coignard, B., Levy-Bruhl, D., & Investigation Team. (2020). First cases of coronavirus disease 2019 (COVID-19) in France: surveillance, investigations and control measures, January 2020. *Eurosurveillance*, 25(6), 200009. doi: 10.2807/1560-7917.ES.2020.25.6.2000094

Thevenet, P., Shen, Y., Maupetit, J., Guyon, F., Derreumaux, P., & Tuffery, P. (2012). PEP-FOLD: an updated de novo structure prediction server for both linear and disulfide bonded cyclic peptides. *Nucleic Acids Research*, 40, 288-293. doi: 10.1093/nar/gks419

Walls, A. C., Park, Y. J., Tortorici, M. A., Wall, A., McGuire, A. T., & Veesler, D. (2020). Structure, Function, and Antigenicity of the SARS-CoV-2 Spike Glycoprotein. *Cell*, 180(2), 1-12. doi: 10.1016/j.cell.2020.02.058

Walls, A. C., Xiong, X., Park, Y. J., Tortorici, M. A., Snijder, J., Quispe, J., Cameroni, E., Gopal, R., Dai, M., Lanzavecchia, A., Zambon, M., Rey, F. A., Corti, D., & Veesler, D. (2019). Unexpected Receptor Functional Mimicry Elucidates Activation of Coronavirus Fusion. *Cell*, 176(5), 1026-1039. doi: 10.1016/j.cell.2018.12.028

Weiss, S. R., & Leibowitz, J. L. (2011). Coronavirus pathogenesis. *Advances in Virus Research*, 81, 85-164. doi: 10.1016/B978-0-12-385885-6.00009-2

Yang, D., & Leibowitz, J. L. (2015). The structure and functions of coronavirus genomic 3' and 5' ends. *Virus Research*, 206, 120-133. doi: 10.1016/j.virusres.2015.02.025

Zaki, A. M., Boheemen, S. V., Bestebroer, T. M.,

Osterhaus, A. D. M. E., & Fouchier, R. A. M. (2012). Isolation of a novel coronavirus from a man with pneumonia in Saudi Arabia. *New England Journal of Medicine*, 367(19), 1814-1820. doi: 10.1056/NEJMoa1211721

Zhang, L., Lin, D., Sun, X., Curth, U., Drosten, C., Sauerhering, L., Becker, S., Rox, K., & Hilgenfeld, R. (2020). Crystal structure of SARS-CoV-2 main protease provides a basis for design of improved α-ketoamide inhibitors. *Science*, 368(6489), 409-412. doi: 10.1126/science.abb3405

Zhao, Z., Hong, W., Zeng, Z., Wu, Y., Hu, K., Tian, X., Li, W., & Cao, Z. (2012). Mucroporin-M1 inhibits hepatitis B virus replication by activating the mitogen-activated proteinkinase (MAPK) pathway and down-regulating HNF4α in vitro and in vivo. *Journal of Biological Chemistry*, 287(36), 30181-30190. doi: 10.1074/jbc.M112.370312

Zhu, N., Zhang, D., Wang, W., Li, X., Yang, B., Song, J., Zhao, X., Huang, B., Shi, W., Lu, R., Niu, P., Zhan, F., Ma, X., Wang, D., Xu, W., Wu, G., Gao, G. F., Tan, W., & China Novel Coronavirus Investigating, Research Team. (2020). A Novel Coronavirus from Patients with Pneumonia in China, 2019. *New England Journal of Medicine*, 382(8), 727-733. doi: 10.1056/NEJMoa2001017